- **Case $\varepsilon = 0$.** This case was studied in [23]. Eq. (A-3) has two roots, 0 and $\frac{3\sqrt{3}}{2}\lambda$. The bifurcation diagram for $\varepsilon = 0$ is shown in Fig. 5.
  - If $\mu < 0$, $(x = 0, y = 0)$ is a stable node.
  - If $0 < \mu < \frac{3\sqrt{3}}{2}\lambda$, the three equilibria corresponding to $x = 0$, $(x = 0, y = 0)$ and $(x = 0, y = \pm\sqrt{\mu})$, are source and saddles respectively. If $x = \pm\sqrt{\mu}$, the polynomials $p_\pm$ have unique roots, $\mp\phi_1(\mu)$, respectively. The corresponding equilibria of system (5), $(x = \sqrt{\mu}, y = -\phi_1(\mu))$ and $(x = -\sqrt{\mu}, y = \phi_1(\mu))$, are stable nodes. Note that $\phi_1(\mu) > \frac{\mu}{3}$ as is clear from Fig. 25.
  - If $\mu > \frac{3\sqrt{3}}{2}\lambda$, system (5) acquires two additional stable equilibria, because the polynomials $p_+(y)$ and $p_-(y)$ acquire an additional pair of roots, $\phi_2(\mu)$, $\phi_3(\mu)$ and $-\phi_2(\mu)$, $-\phi_3(\mu)$, respectively. Fig. 25 shows that $0 < \phi_2(\mu) < \sqrt{\frac{\mu}{3}}$, while $\phi_3(\mu) > \sqrt{\frac{\mu}{3}}$. The equilibria $(x = \sqrt{\mu}, y = \phi_2(\mu))$ and $(x = -\sqrt{\mu}, y = -\phi_2(\mu))$ are saddles, while $(x = \sqrt{\mu}, y = \phi_3(\mu))$ and $(x = -\sqrt{\mu}, y = -\phi_3(\mu))$ are stable nodes.
- **Case $0 < \varepsilon < \lambda$.** The bifurcation diagram for this case is exemplified by the one for $\varepsilon = 0.8$ in Fig. 5. Eq. (A-3) has two roots, $\mu_1^*(\varepsilon)$ and $\mu_2^*(\varepsilon)$. The qualitative behavior of $p_+(y)$ and $p_-(y)$ for at various $\mu > 0$ for $0 < \varepsilon < skip\lambda$ is shown in Fig. 26. The root $\mu_1^*(\varepsilon)$ tends

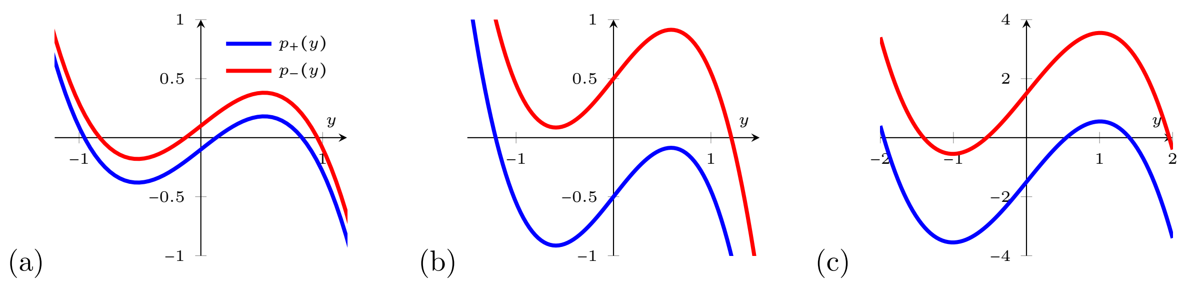

Figure 26: The qualitative behavior of the polynomials $p_+(y)$ and $p_-(y)$ as μ increases from 0 to $+\infty$ fixed $\lambda > 0$ and $0 < \varepsilon < \lambda$. (a): $p_+(y)$ and $p_-(y)$ have three roots at $\mu < \mu_1^*(\varepsilon)$. (b): Unique roots at $\mu_1^*(\varepsilon) < \mu < \mu_2^*(\varepsilon)$. (c): Three roots at $\mu < \mu_2^*(\varepsilon)$. $\mu_1^*(\varepsilon)$ and $\mu_2^*(\varepsilon)$ are the two roots of (A-3) at $0 \le \varepsilon \le \lambda$. Here, $\lambda = 1$, $\varepsilon = 0.8$, and $\mu = 0.01$ (a), $\mu = 0.5$ (b), and $\mu = 1.5$ (c).

to zero as $\varepsilon \to 0$. This means that the interval of $0 < \mu < \mu_1^*(\varepsilon)$ where three roots pf $p_+(y)$ and $p_-(y)$ exist is short. To find how $\mu_1^*(\varepsilon)$ scales with ε and λ, we recast Eq. (A-3) as a cubic equation with respect to $t := \mu^{1/3}$:

$$t^3 - at + b = 0, \quad \text{where} \quad a := \left(\frac{3\sqrt{3}\lambda}{2}\right)^{2/3}, \quad b = \varepsilon. \tag{A-6}$$

Its roots are given by Viete's trigonometric formula [41]

$$t_k = 2\sqrt{\frac{a}{3}}\cos\left[\frac{1}{3}\arccos\left(-\frac{3b}{2a}\sqrt{\frac{3}{a}}\right) + \frac{2\pi k}{3}\right], \quad k = 0, 1, 2. \tag{A-7}$$

The roots corresponding to $k = 0, 1$ tend, respectively, to $\pm\sqrt{a}$, while the root corresponding to $k = 2$ tends to zero as $b \equiv \varepsilon \to 0$. Taylor-expanding the root t_2 at $\varepsilon = 0$ we find

$$\mu_1^*(\varepsilon) \approx \frac{4\varepsilon^3}{27\lambda^2}. \tag{A-8}$$

Cf. the inset of Fig. 25(b). If this value of μ is much less than $\mu_1^*(\varepsilon)$, the following approximation for the three roots of $p_+(y)$ are obtained by Taylor-expanding Viete's formula (A-7) with $a = \mu + \varepsilon$ and $b = \lambda\sqrt{\mu}$ and treating μ as a small positive parameter:

$$y_{0,1}^* = \pm\sqrt{\varepsilon} - \frac{\lambda\sqrt{\mu}}{2\varepsilon} + O(\mu^{3/2}), \quad y_2^* = \frac{\lambda\sqrt{\mu}}{\varepsilon} + O(\mu^{3/2}). \tag{A-9}$$

– If $\mu < -\varepsilon$, $(x = 0, y = 0)$ is the only equilibrium of system (5), and it is a stable node.
– If $-\varepsilon < \mu < 0$, system (5) has three equilibria: two stable nodes $(x = 0, y = \pm\sqrt{\varepsilon + \mu})$ and a saddle $(x = 0, y = 0)$.
– If $\mu > 0$, the equilibria $(x = 0, y = 0)$ and $(x = 0, y = \pm\sqrt{\mu + \varepsilon})$ are source and saddles respectively. Let $x = \pm\sqrt{\mu}$. Then the polynomials $p_\pm(y)$ have three roots if $0 < \mu < \mu_1^*(\varepsilon)$ or $\mu > \mu_2^*(\varepsilon)$, and one root if $\mu_1^*(\varepsilon) < \mu < \mu_2^*(\varepsilon)$. The eigenvalues $\mu + \varepsilon - 3y^2$ of J in Eq. (9), corresponding to y, are negative if $y = \pm\phi_1(\mu)$ or $y = \pm\phi_3(\mu)$, as $\phi_1(\mu), \phi_3(\mu) > \sqrt{\frac{\mu+\varepsilon}{3}}$, and these eigenvalues are positive if $y = \pm\phi_2(\mu)$ – see Fig. 25(a). Hence, the equilibria $(x = \sqrt{\mu}, y = -\phi_1(\mu))$, $(x = \sqrt{\mu}, y = -\phi_3(\mu))$, $(x = -\sqrt{\mu}, y = \phi_1(\mu))$, and $(x = -\sqrt{\mu}, y = -\phi_3(\mu))$ are stable nodes, while the equilibria $(x = \sqrt{\mu}, y = \phi_2(\mu))$ and $(x = -\sqrt{\mu}, y = -\phi_2(\mu))$ are saddles. A similar equilibrium stability structure occurs at $\mu > \mu_2^*(\varepsilon)$. If $\mu_1^*(\varepsilon) < \mu < \mu_2^*(\varepsilon)$, $p_\pm(y)$ have unique roots $\mp\phi_1(\mu)$, respectively. The corresponding equilibria of system (5), $(x = \sqrt{\mu}, y = -\phi_1(\mu))$ and $(x = -\sqrt{\mu}, y = \phi_1(\mu))$, are stable nodes.

- **Case $\boldsymbol{\varepsilon > \lambda}$.** Eq. (A-3) has no roots. The polynomials $p_+(y)$ and $p_-(y)$ have three roots at all $\mu > 0$, and the schematic in Fig. 25 (a) applies. A typical bifurcation diagram for this case is like the one for $\varepsilon = 1.2$ in Fig. 5. If $\mu < 0$, $x = 0$ is the only equilibrium of the first cell, and the structure and stability of equilibria of system (5) are the same as in the previous case. If $\mu > 0$, the polynomials $p_\pm(y)$ have three roots at all $\mu > 0$. The structure and stability of the equilibria of system (5) are the same as in the previous case with $0 < \mu < \mu_1^*(\varepsilon)$ and $\mu > \mu_2^*(\varepsilon)$.
- **Case $\boldsymbol{\varepsilon < 0}$.** If $\varepsilon < 0$, $p_+(y)$ and $p_-(y)$ are monotonously decreasing at $\mu \to 0+$. The steady-state bifurcation from one to three equilibria occurs at the only root $\mu^*(\varepsilon)$ of Eq. (A-3) at $\varepsilon < 0$. A bifurcation diagram for this case is exemplified by the one for $\varepsilon = -0.8$ in Fig. 5. If $0 < \mu < \mu^*(\varepsilon)$, the polynomials $p_\pm(y)$ have unique roots $\mp\phi_1(\mu)$, respectively. The structure and stability of the equilibria of system (5) are the same as in the case $0 < \varepsilon < \lambda$ with $\mu_1^*(\varepsilon) < \mu < \mu_2^*(\varepsilon)$. If $\mu > \mu^*(\varepsilon)$, the polynomials $p_\pm(y)$ have three roots, whose structure and stability are the same as in the case $0 < \varepsilon < \lambda$ with $\mu > \mu_2^*(\varepsilon)$.

B Proof of Proposition 1

Proof. 1. Eq. (24) can be rewritten as

$$|v|^2 = \frac{1}{\tilde{\mu}^2(1 - |v|^2)^2 + \tilde{\sigma}^2}. \tag{B-10}$$

The right-hand side of Eq. (B-10) is the function of $|v|^2$ known as the "Witch of Agnesi". This function is positive, symmetric with respect to $|v|^2 = 1$, and reaches its unique extremum, the maximum $|\sigma|^{-2} \geq 1$, at $|v|^2 = 1$. Since the Witch of Agnesi is strictly decreasing on $|v|^2 \geq 1$, and $f(|v|^2) = |v|^2$ is strictly increasing on $[1, \infty)$, there exists a unique solution on $[1, \infty)$ – see Fig. 27(a). Up to two additional solutions may exist on $(0, 1)$ – see Fig. 27(b). Note that if $\tilde{\sigma} = 0$, the graph of the Witch of Agnesi acquires a vertical asymptote at $|v|^2 = 1$, but the same argument applies.

Once $|v|^2$ is found, v_R and v_I are uniquely determined from Eq. (23):

$$v_R = \frac{\tilde{\mu}(1 - |v|^2)}{\tilde{\mu}^2(|v|^2 - 1)^2 + \tilde{\sigma}^2}, \quad v_I = -\frac{\tilde{\sigma}}{\tilde{\mu}^2(1 - |v|^2)^2 + \tilde{\sigma}^2} \tag{B-11}$$

Note that if $|v|^2 = 1$, then $|\sigma| = 1$, $v_R = 0$, and $v_I = -\mathrm{sgn}(\tilde{\sigma})$.

To assess the stability of the solution with $|v|^2 \geq 1$, we write out the Jacobian of Eq. (22):

$$J(v_R, v_I) = \begin{bmatrix} \tilde{\mu}(1 - |v|^2) - 2\tilde{\mu}v_R^2 & -\tilde{\sigma} - 2\tilde{\mu}v_I v_R \\ \tilde{\sigma} - 2\tilde{\mu}v_R v_I & \tilde{\mu}(1 - |v|^2) - 2\tilde{\mu}v_I^2 \end{bmatrix}. \tag{B-12}$$

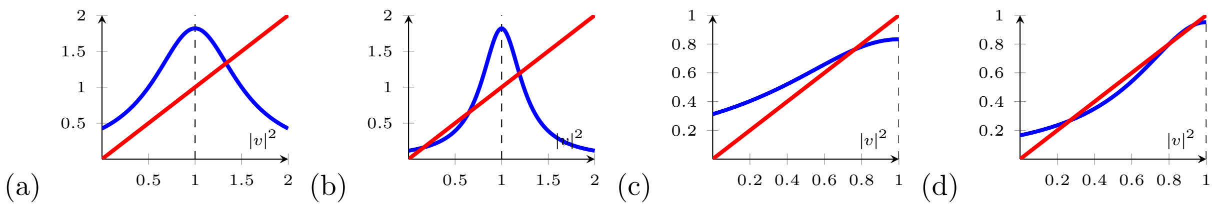

Figure 27: The structure of roots of Eq. (B-10) depending n $\tilde{\mu}$ and $\tilde{\sigma}$. If $|\tilde{\sigma}| \le 1$, then Eq. (B-10) has a unique root on $[1, \infty)$. If $\tilde{\mu}$ is small enough, this is the only root of Eq. (B-10) as in (a). If $\tilde{\mu}$ is large enough, Eq. (B-10) has two additional roots on $(0, 1)$ as in (b). If $|\sigma| > 1$, then Eq. (B-10) has at least one and up to three roots on $(0, 1)$, as in (c) and (d), respectively.

The conditions for the asymptotic stability are

$$\det J = \tilde{\mu}^2(1 - |v|^2)(1 - 3|v|^2) + \tilde{\sigma}^2 > 0, \tag{B-13}$$

$$\operatorname{tr} J = 2\tilde{\mu}(1 - 2|v|^2) < 0. \tag{B-14}$$

We note that $|v|^2 = 1$ implies $|\sigma| = 1$. Then $\det J > 0$ and $\operatorname{tr} J < 0$ if $|v|^2 \ge 1$. This completes the proof of statement (1).

2. Statement (2) follows from the expansion of the left-hand side of Eq. (24) at $\tilde{\sigma} = 0$:

$$|v|^6 - 2|v|^4 + |v|^2 = \frac{1}{\tilde{\mu}^2}. \tag{B-15}$$

Letting $\tilde{\mu} \to 0$ and observing that the term $\tilde{\mu}^2|v|^6$ dominates the left-hand side of Eq. (B-15), we obtain that $|v| \approx \tilde{\mu}^{-1/3}$.

3. Given $|v|^2 \in (0, +\infty)$, $\tilde{\sigma} \in \mathbb{R}$, and $\tilde{\mu} > 0$ uniquely define an equilibrium (v_R, v_I) of ODE (22) by Eq. (B-11), provided that $(\tilde{\sigma}, \tilde{\mu})$ lie on the ellipse (24). This equilibrium is asymptotically stable if and only if inequalities (B-13)–(B-14) hold. Hence, we are seeking the region in the $(\tilde{\sigma}, \tilde{\mu})$-space where the system

$$|v|^2\tilde{\sigma}^2 + |v|^2(1 - |v|^2)^2\tilde{\mu}^2 = 1, \tag{B-16}$$

$$\tilde{\mu}^2(1 - |v|^2)(1 - 3|v|^2) + \tilde{\sigma}^2 > 0, \tag{B-17}$$

$$2\tilde{\mu}(1 - 2|v|^2) < 0, \tag{B-18}$$

is compatible. By Statement (1), the sought region includes the strip $\tilde{\sigma}^2 \le 1$, corresponding to the range $|v|^2 \in [1, \infty)$. Hence, it remains to examine the region $|v|^2 \in (0, 1)$. Eq. (B-18) implies that $|v|^2 > \frac{1}{2}$, which means that the region spanned by the family of ellipses (B-16) with $|v|^2 \in (\frac{1}{2}, 1)$ includes the part of the sought region lying beyond the strip $\tilde{\sigma}^2 \le 1$. Below, we will find the part of this region with $\tilde{\sigma} > 1$. Its other part with $\tilde{\sigma} < -1$ is obtained by a mirror reflection with respect to the axis $\tilde{\sigma} = 0$.

At each fixed $\tilde{\mu}^2 > 0$, we seek the largest $\tilde{\sigma}^2$ satisfying Eq. (B-16):

$$\tilde{\sigma}^2 = \frac{1}{|v|^2} - (1 - |v|^2)^2\tilde{\mu}^2 \ \to \ \max, \quad \frac{1}{2} < |v|^2 < 1.$$

Denoting $|v|^2$ by x, taking the derivative $\frac{d(\tilde{\sigma}^2)}{dx}$ and setting it to zero, we find that the interior point extrema of $\tilde{\sigma}^2$ exist if and only if the equation

$$\tilde{\mu}^2 = \frac{1}{2x^2(1 - x)} \tag{B-19}$$

has roots, which is the case if $\tilde{\mu}^2 \ge \frac{27}{8}$. If $\tilde{\mu}^2 > \frac{27}{8}$, Eq. (B-19) has two positive roots, one greater than $\frac{2}{3}$, that corresponds to a local maximum of $\tilde{\sigma}^2$, and one less than $\frac{2}{3}$, that